

## Selective Intercalation of Cs<sup>+</sup> in the “V”-Shaped Cavity of a Bichromophoric Anion Radical: Cs<sup>+</sup> Assisted $\pi$ -s- $\pi$ -Delocalization of an Electron

Cheryl D. Stevenson,<sup>\*,†</sup> Matthew K. Kiesewetter,<sup>†</sup> Richard C. Reiter,<sup>†</sup> Vincent J. Chebny,<sup>‡</sup> and Rajendra Rathore<sup>\*,‡</sup>

Department of Chemistry, Illinois State University, Normal, Illinois 61790-4160, and Department of Chemistry, Marquette University, P.O. Box 1881, Milwaukee, Wisconsin 53201-1881

Received: April 21, 2006; In Final Form: June 9, 2006

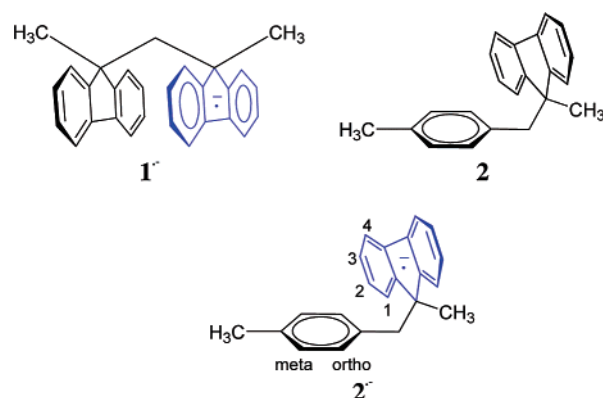
EPR studies in tetrahydrofuran, reveal that the one electron reduction of 1-(9-methyl-9H-fluoren-9-yl)-4-methylbenzene via electron transfer from cesium metal produces an anion radical that has a large affinity for the cesium cation. The affinity of this anion radical for Cs<sup>+</sup> is so great that it will actually “suck” the Cs<sup>+</sup> (but not Na<sup>+</sup> or K<sup>+</sup>) right out of the grasp of 18-crown-6, leading to a cation-assisted  $\pi$ -stacked complex, where the s-orbital of the metal cation is simultaneously overlapped with the  $\pi$ -clouds of the phenyl and fluorenyl moieties. At ambient temperature, proton- and cesium-electron coupling constants are rapidly (on the EPR time scale) modulated as a result of the simultaneous existence of two interconverting conformers having an averaged cesium splitting ( $a_{Cs}$ ) of about 1.6 G. The  $\pi$ -s- $\pi$ -electronic coupling can be turned on or off via the addition or removal of cesium cations. Analogous  $\pi$ -s- $\pi$ -electronic coupling is observed in the 1,4-bis(9-methyl-9H-fluoren-9-yl)benzene-cesium system.

### Introduction

$\pi$ -Stacking is very important and is of extreme contemporary interest,<sup>1</sup> in part due to its significance in DNA chemistry,<sup>2</sup> and in the concept of molecular electronics.<sup>3</sup> In molecular systems containing a hole or an extra electron,  $\pi$ -stacking can lead to spin and charge delocalization between otherwise isolated  $\pi$ -moieties,<sup>4</sup> the quintessential example being para-cyclophane,<sup>5</sup> Figure 1. Intercalators, molecules inserted between two  $\pi$ -facing moieties (e.g., base pairs in DNA), can perturb the  $\pi$ -stacking interactions. In view of these facts, we envisioned anion radical systems with isolated  $\pi$ -moieties that could accept a properly fitted cation, which would activate conjugative interaction between these two moieties, Figure 1.

The one electron reduction of di-fluorene (**1**) results in the formation of the corresponding anion radical (**1**<sup>•-</sup>), where all of the electron spin resides on just one of the fluorene moieties, Figure 2.<sup>6,7</sup> Attempts to insert a cation between the two fluorene units have failed, expectedly, due to the close van der Waals contact between the cofacially juxtaposed fluorene moieties.<sup>7c</sup> Such a restriction is relieved in the hydrocarbon 1-(9-methyl-9H-fluoren-9-yl)-4-methylbenzene (**2**), which contains two aromatic moieties and a “V”-shaped cavity especially efficacious for trapping cations. Hence, we were motivated to investigate the possibility of inserting a cation between the fluorenyl and xylenyl moieties of **2**<sup>•-</sup> which would, in turn, produce an electron delocalization throughout these two moieties.

The B3LYP/6-31G\* (a protocol that has worked well for anion radical systems)<sup>8</sup> calculated distance between the two ortho carbons on the fluorene and the nearest phenyl ortho carbons in the “V”-shaped cavity of **2**<sup>•-</sup> is 3.50 Å. Consequently, it was anticipated that the first three alkali metal cations would



be too small to physically bridge the gap between the two isolated  $\pi$ -systems. The Pauling ionic radius of Cs<sup>+</sup> is 1.69 Å, which should be about perfect to bridge the gap to complete an effective overlap of the unoccupied s-orbital of Cs<sup>+</sup> with the  $\pi$ -orbitals of both moieties of the anion radical.

It was anticipated that this near perfect fit would manifest itself in the EPR spectrum of Cs<sup>+</sup> > **2**<sup>•-</sup>, exhibiting delocalization of the spin and charge over both the fluorenyl and xylenyl moieties. In this molecular syllogistic logic gate, the presence of the larger alkali metal cations will act as the “if” provider and the “then” consequence will be the observation of spin density drainage from the fluorenyl to the xylenyl  $\pi$ -system (s-orbital assisted electronic coupling).

### Results and Discussion

The reduction of **2**, with potassium or sodium metal, in THF-containing 18-crown-6 (added to prevent the complexities of normal ion association and ion aggregation) yields a solution exhibiting a very weak EPR signal. The anion radical concentration is extremely small, but the EPR pattern is nearly identical to that observed for **1**<sup>•-</sup>, which, in turn, is the same as that

\* To whom correspondence should be addressed. E-mail: cdsteve@ilstu.edu and rajendra.rathore@marquette.edu.

<sup>†</sup> Illinois State University.

<sup>‡</sup> Marquette University.

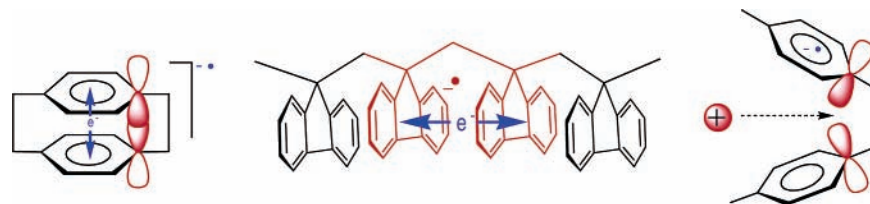


**Figure 1.** (Left) The  $\pi$ -stacked anion radical of para-cyclophane allowing complete conjugation of the added electron throughout both ring systems. (Middle) The  $\pi$ -stacking of the two central fluorene moieties allowing the odd electron to undergo very rapid exchange between two central fluorene rings. (Right) An “open” anion radical, with one  $\pi$ -moiety reduced and the other in the neutral state. A properly sized cation, however, could insert itself, via Coulombic attraction, and complete the conjugative stack (circuit) by simultaneously overlapping with the p-orbitals of both  $\pi$ -systems (a  $\pi$ -s- $\pi$ -stack).

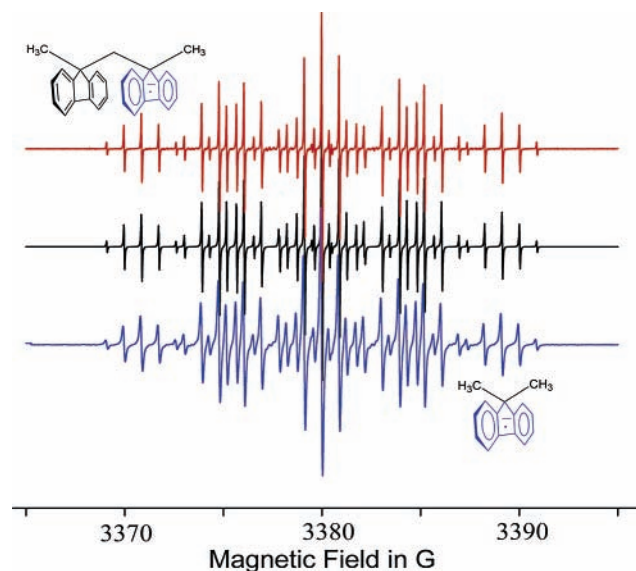


**Figure 2.** (Upper) X-band EPR spectrum  $1^{\bullet-}$  in the absence of ion association. This spectrum is nearly identical to that for the anion radical of dimethylfluorene (Lower). (Middle) A computer-generated simulation using coupling constants of 0.88 G (4Hs), 3.941 G (2Hs), and 5.20 G (2Hs).

observed for the anion radical of dimethylfluorene, Figure 1. The EPR spectra of  $1^{\bullet-}$  and  $2^{\bullet-}$  are exactly as anticipated for systems where the spin and charge densities are delocalized over a single fluorene moiety.<sup>6,7</sup> However, the amount of anion radical that is generated is extremely small, meaning that  $2^{\bullet-}$  is very labile under these conditions. Further, the broad resonance for a “living polymer”<sup>9</sup> is evident in these spectra.

The reduction of **2** with Rb metal in a THF solution containing excess 18-crown-6 results a strong well-resolved EPR spectrum, Figure 3. As in the case of  $1^{\bullet-}$ , the odd electron interaction is with a fluorenyl moiety only. This is similar to the cases of the K and Na systems, but the spin distribution is very different and the anion radical concentration (as evidenced by the intensity of the EPR signal) is much larger. We assign to this species a structure where the Rb cation is interacting strongly with the fluorenyl moiety; strong couplings from both isotopes of Rb ( $^{85}\text{Rb}$  and  $^{87}\text{Rb}$ ) are present. Clearly the xylenyl unit is perturbing the spin distribution, and nearly simultaneous interaction with both  $\pi$ -systems is helping to stabilize the anion radical ( $\text{Rb}^+ > 2^{\bullet-}$ ). This experiment, while not quite yielding the full delocalization hoped for, leads to optimism for the Cs system, because the  $\text{Rb}^+$  has clearly been extracted from the grasp of the crown ether by  $2^{\bullet-}$ .

Electron transfer, in THF containing an excess of 18-crown-6, to **2** from Cs metal results in a solution yielding a strong enduring EPR signal at 25 °C, showing that the odd electron is interacting strongly with the cesium ion and is delocalized over both  $\pi$ -systems, Figure 4. The affinity of the anion radical of **2**

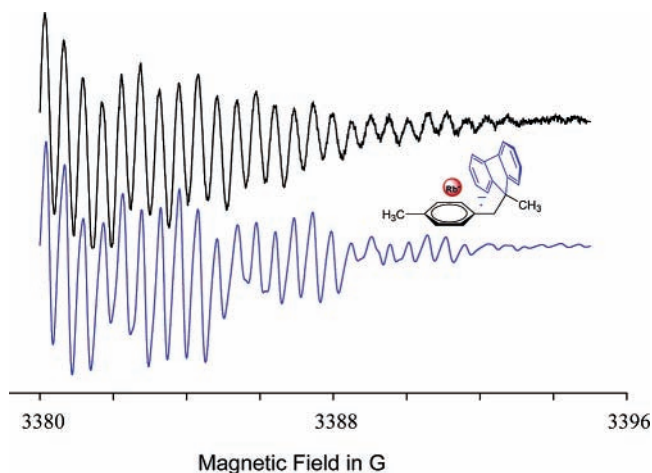


**Figure 3.** (Upper) High-field half of the ambient temperature x-band EPR spectrum of  $^{85}\text{Rb}^+ > 2^{\bullet-}$  and  $^{87}\text{Rb}^+ > 2^{\bullet-}$  in their natural abundance isotopic ratio in THF containing excess 18-crown-6. (Lower) A computer-generated simulation generated using  $a_{85\text{Rb}}$  and  $a_{87\text{Rb}}$  values of 0.505 and 1.69 G, respectively, and  $a_{\text{HS}}$  of 3.64 (4Hs) and 3.12 (4Hs). A single line for the “living polymer” was included near the spectral center.<sup>9</sup>

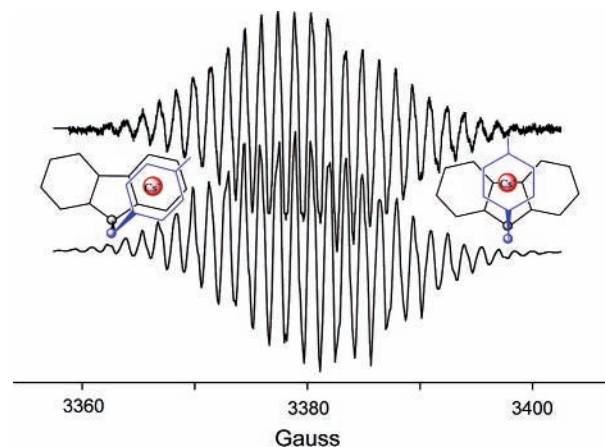


**Figure 4.** (Upper) X-band EPR spectrum of a sample of **2** reduced with Cs metal in THF containing excess 18-crown-6 and recorded at 298 K. (Lower) Computer-generated simulation based upon the two structures shown as explained in the text.

for  $\text{Cs}^+$  is so great that it extracts  $\text{Cs}^+$  right out of the grasp of 18-crown-6, leading to the cation-assisted electronic coupling between the fluorene and xylene moieties in  $\text{Cs}^+ > 2^{\bullet-}$ . More careful inspection of the spectrum reveals rapid (on the EPR time scale) modulation of the couplings. The modulation of the electron–Cs and electron–proton couplings appears to be a result of the simultaneous existence of two rapidly interconverting conformers having an averaged cesium splitting ( $a_{\text{Cs}}$ ) of about 1.6 G.

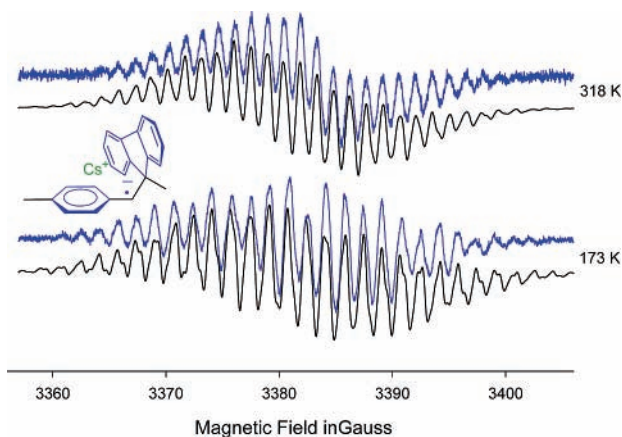
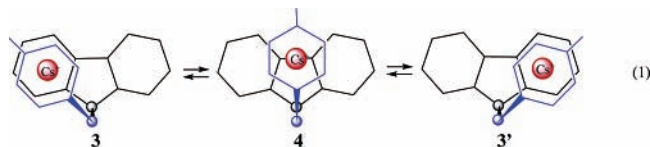


**Figure 5.** X-band EPR spectra (blue) and their computer simulations (black), taken after the reduction of **2** in THF containing an excess of 18-crown-6. The upper spectrum was recorded at 318 K and exhibits coupling constants of  $a_{Cs} = 1.5$  G (1Cs),  $a_H = 4.33$  G (4 phenyl Hs, assigned via deuteration studies),  $a_H = 3.10$  G (4Hs), and  $a_H = 2.57$  G (4Hs). The lower spectrum was recorded at 173 K and exhibits coupling constants of  $a_{Cs} = 1.70$  G (1Cs),  $a_H = 4.90$  G (4 phenyl Hs),  $a_H = 3.67$  G (4Hs), and  $a_H = 3.05$  G (4Hs).

The time-averaged proton splittings originate from three groups of four Hs. Each group of four is likely comprised of two pairs, similar enough to be indistinguishable given the large line width. The line widths make it clear that these splittings are really average splittings from a rapid interchange between two molecular morphologies (vide infra). In any case, the odd electron couples to twelve protons on  $sp^2$  hybridized carbons. Consistent with this observation is the anion radical of paraxylene, where the  $a_H$  for the four ring protons is 5.39 G, and the methyl protons are not resolved but contribute to the line-width.<sup>10</sup> In the case of  $Cs^+ > 2^{\bullet-}$ , the splittings from the  $\beta$  protons are, likewise, not resolved and simply contribute to the line-widths of the individual hyperfine components.

To gain an understanding of the line-width modulation effects, EPR spectra of  $Cs^+ > 2^{\bullet-}$  were recorded at successively lower temperatures until the signal no longer changed. At  $-100$  °C, a single conformer (**3**) is observed, Figure 5 (lower). At  $+45$  °C, the second conformer (**4**) can be seen, Figure 5 (upper). Both raising and lowering the temperature reduces the intensity of the EPR signal. However, the EPR spectra for both the high and low temperature conformers could be simulated, each in terms of 12 protons and one  $Cs^+$  but with very different coupling constants, Figure 5. With the spectral parameters for **3** and **4** in hand, we added their two computer simulations together in a ratio of  $[3]/[4] = 0.4$  and reproduced the  $25$  °C experimental spectrum of  $2^{\bullet-}, Cs^+$  by allowing rapid exchange between **3** and **4** (eq 1) to take place, Figure 4. The shape of the simulation is very sensitive to the rate of interchange between the two position conformers. The forward and reverse rate constants (for eq 1) are  $7.0 \times 10^7$  and  $1.8 \times 10^8$   $s^{-1}$ , respectively.



Because the  $Cs^+$  ion acts as a  $\pi$ -conduit between the isolated xylenic and fluorenyl  $\pi$ -systems, and **3** and **4** have different cesium couplings, their structures, based on B3LYP calculations of the neutral materials, are assigned above in eq 1. The interconversion between **3**, **4**, and **3'** requires a simple C–C

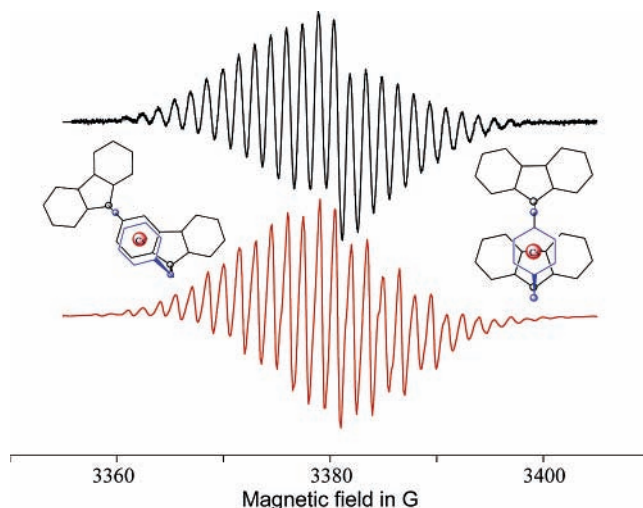
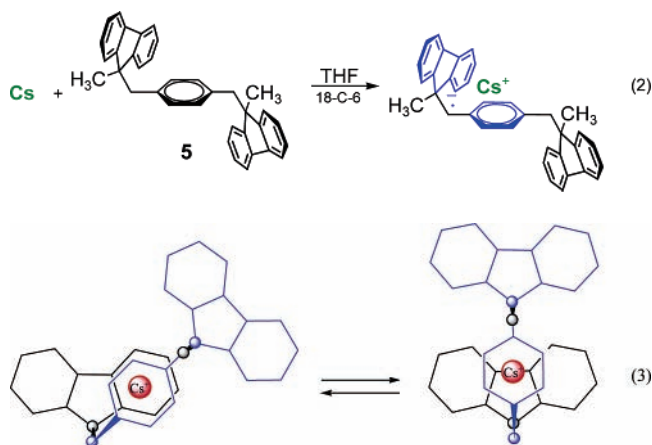


**Figure 6.** (Upper) X-band EPR spectrum of a sample of **5** reduced with Cs metal in THF containing excess 18-crown-6 and recorded at 298 K. (Lower) A computer simulation generated by dynamic mixing of the simulations for the spectra shown in Figure 5. The same coupling constants described in Figure 5 were used to generate this simulation. The simulation profiles eq 3, where  $K_{eq} = 0.25$  and  $k_{(forward)} = 2.5 \times 10^7$   $s^{-1}$ .

bond rotation and, thus, can be readily achieved by simple temperature modulation.

Under the same conditions, the Cs reduction of 1,4-bis(9-methyl-9H-fluoren-9-yl)benzene (**5**) resulted in the formation of an anion radical that reveals an EPR spectrum that is very similar to that of  $2^{\bullet-}$  (shown in Figure 4). Hence, unlike the previously observed symmetric encapsulation of  $Ag^+$  by **5**,<sup>11</sup> the anion radical of **5** encapsulates  $Cs^+$  and localizes it on one side of the molecule, eq 2. Of course, the ambient temperature EPR pattern for  $5^{\bullet-}, Cs^+$  is nicely simulated via the dynamic mixing (eq 3) of the simulations for **3** and **4**, Figure 6.



As it remained unproven which proton splittings represented those from the phenyl moiety and which from the fluorenyl moiety, the experiment was carried out with **5-d<sub>16</sub>** (fluorenyl moiety deuterated).<sup>13</sup> Four proton splittings with a time averaged  $a_H$  of about 4.5 G coupled with the smaller deuterium splittings ( $\gamma_H/\gamma_D = 6.54$ ) account for the observed total spectral width. Again, the rapid molecular interchange (eq 1) causes obvious line-width modulation, Figure 7. The four large splittings and, hence, spin densities exist in the xylenyl moiety, as predicted in eq 1. The spectrum was simulated using the same averaged coupling constants as described in Figure 5, but the line width modulation effects could not be included due to the

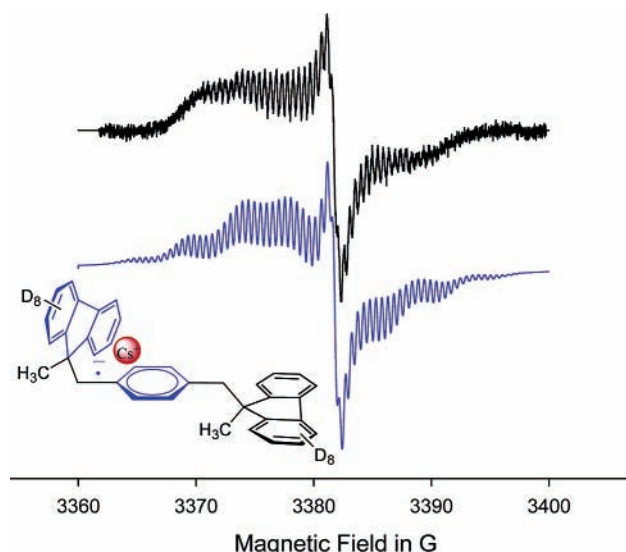


**Figure 7.** (Upper) Ambient temperature x-band EPR spectrum of Cs<sup>+</sup> > **5-d<sub>16</sub><sup>+</sup>**, at 298 K in THF containing excess 18-crown-6. (Lower) A computer simulation generated without the inclusion of the line width effects ( $k$  for eq 1 was assumed to be 0) that modulate the Cs, D, and H coupling constants. Single lines for the “living polymers” were included near the spectral center.<sup>9</sup> Note how the lines broaden to oblivion at the low and high field extremes of the real spectrum but not in the simulation. This figure renders the line width modulation effects obvious; of the 8 Cs hyperfine lines, the broadening for the  $m = +7/2$  and  $-7/2 > m = +5/2$  and  $-5/2 > m = +3/2$  and  $-3/2 > m = +1/2$  and  $-1/2$ .

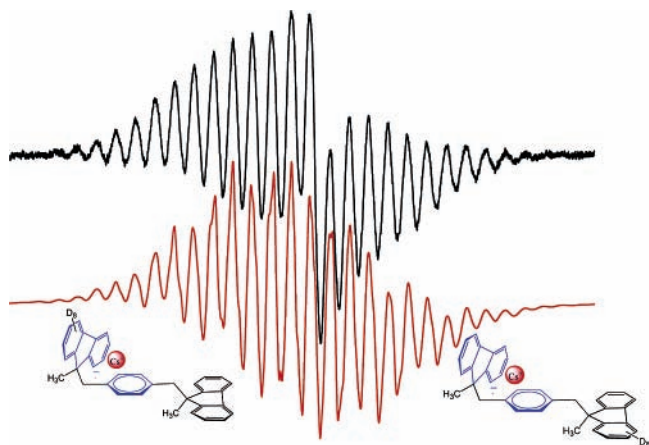


**Figure 8.** Scan (45 G) of an x-band EPR spectrum of **5-d<sub>8</sub>** reduced with Cs metal 298 K with the corresponding computer-generated simulation shown below. The simulation was generated using the parameters described in Figure 5, except that the  $a_{DS}$  were calculated using  $\gamma_H/\gamma_D = 6.54$ . A smaller amount (43%) of the material with the electron located on the deuterated side was included. This smaller amount is due to the deuterium equilibrium isotope effect; see: Stevenson, C. D.; Espe, M. P.; Reiter, R. C. *J. Am. Chem. Soc.* **1986**, 108, 5760.

limitations of our simulation program. Further, no other program, to our knowledge, can handle this degree of complexity.

To provide demonstrative proof that the cesium cation is only interacting with one fluorenyl moiety, we reduced **5-d<sub>8</sub>**, where all of the hydrogens on sp<sup>2</sup> hybridized carbons on only one fluorenyl moiety are replaced with deuteriums. This experiment produced a THF solution exhibiting an EPR spectrum that is similar to that obtained from the Cs reduction of **5**, Figure 8.

In summary, we have demonstrated that **2** and **5**, containing “V”-shaped cavities, produce anion radicals in which a preferential Cs<sup>+</sup> intercalation in the “V”-shaped cavity promotes

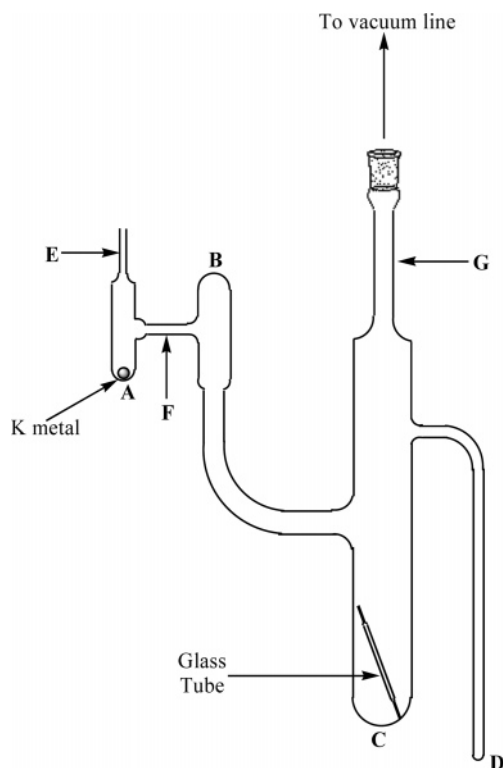


**Figure 9.** Apparatus used for the generation of the anion radicals.

effective electronic coupling (i.e.,  $\pi$ -s- $\pi$ -interaction) between the isolated aromatic moieties and allows the effective removal of cesium cation from the grasp of 18-crown-6.<sup>12</sup> However, removal of the Cs<sup>+</sup> from the anion radicals of either **2** or **5** results in loss of structural integrities of the anion radical systems. The EPR spectra of Cs-bound anion radicals of **2** and **5** are readily reconciled based on the dynamic structural modulation at room temperature by a simple rotation of a C–C bond connecting the fluorenyl and xylenic ring systems, eq 1. This appears to be an example, involving simple hydrocarbons, that is somewhat analogous to the anionic proteinaceous ion channels that undergo specific conformational changes when in the presence of the appropriately sized K<sup>+</sup> and/or Na<sup>+</sup>.<sup>14</sup>

## Experimental Section

**2** and **5** were synthesized as previously described.<sup>11</sup> A glass tube was charged with 0.1 millimole of **2**, **5** (or their deuterated analogues) and sealed with fragile ends. This tube was then placed into bulb C, along with c.a. 0.3 millimole of 18-crown-6, of the Pyrex glass apparatus shown in Figure 9. A small amount of alkali metal was placed into bulb A, which was then sealed at point E. The entire apparatus was evacuated, and the metal was sublimed into bulb B to form a potassium mirror. Bulb A was sealed from the apparatus at point F. THF (4 mL) was distilled from a separate flask, containing NaK<sub>2</sub> alloy directly into bulb C, and the evacuated apparatus was subsequently sealed from the vacuum line at point G. The apparatus was shaken vigorously to break the glass tube containing the substrate and agitated lightly to dissolve it. The apparatus was then tilted to allow the solution to come into contact with the metal mirror until a highly colored paramagnetic solution persisted.

The EPR spectrum was recorded immediately after reduction by placing the 3-mm tube D into the EPR cavity. The apparatus could be removed from the EPR spectrometer, the solution exposed to more metal, and the spectrum recorded again. This

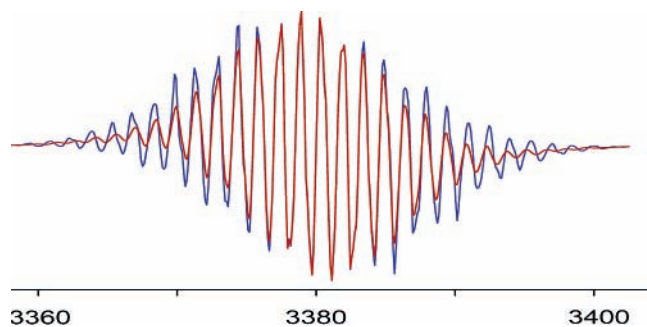


**Figure 10.** Computer simulations generated by dynamic mixing of the simulations for the spectra shown in Figure 5. The simulation profiles eq 1, where  $K_{\text{eq}} = 0.4$  and  $k_{\text{(forward)}} = 7 \times 10^7 \text{ s}^{-1}$  (blue) and  $1.4 \times 10^7 \text{ s}^{-1}$  (red). Figure 4 was generated using a  $k_{\text{(forward)}}$  of  $7 \times 10^7 \text{ s}^{-1}$ .

process was continued to allow monitoring of the EPR signal as a function of added metal. The simulations were carried out using the *EWSIM* software as previously described.<sup>15</sup>

The appearance of the simulations generated by mixing the high and low-temperature spectra, shown in Figure 5 proved to be quite sensitive to the rate constants and equilibrium constants used (for eqs 1 and 3). Simulations generated using  $K_{\text{eq}} = 0.4$  and  $k_{\text{(forward)}} = 7 \times 10^7 \text{ s}^{-1}$  (blue) and  $1.4 \times 10^7 \text{ s}^{-1}$  (red) are shown in Figure 10. There is some interplay between the effects of changing the rate constants and the equilibrium constants; consequently, we were unable to obtain reliable changes in the  $K$ s and  $k$ s as a function of temperature. This precluded the measurements of enthalpies of activation.

**Acknowledgment.** We thank the National Science Foundation and Petroleum Research Funds, administered by the American Chemical Society, for financial support.

#### References and Notes

(1) Coronado, E.; Day, P. *Chem. Rev.* **2004**, *104*, 5419.

(2) Treadway, C. R.; Hill, M. G.; Barton, J. K. *Chem. Phys.*, **2002**, *2–3*, 409.

(3) (a) Petty, M. C.; Bryce, M. R.; Bloor, D., Eds. *Introduction to Molecular Electronics*; Oxford University Press: New York, 1995. Also see: Tour, J. M. *Acc. Chem. Res.* **2000**, *33*, 791 and references therein. (b) Ainsworth, S. J. *Chem. Eng. News* **2004**, *82(15)*, 17. (c) Baum, R. M. *Chem. Eng. News* **2004**, *82(15)*, 3.

(4) For example see: Dutan, C.; Choua, S.; Berclaz, T.; Geoffroy, M.; Mezailles, N.; Moores, A.; Ricard, L.; Le Floch P. *J. Am. Chem. Soc.* **2003**, *125*, 4487.

(5) Gerson, F.; Martin, W. B., Jr. *J. Am. Chem. Soc.* **1969**, *91*, 1883.

(6) (a) Stevenson, C. D.; Kiesewetter, M. K.; Reiter, R. C.; Abdelwahed, S. H.; Rathore R. *J. Am. Chem. Soc.* **2005**, *127*, 5282. (b) Rathore R.; Abdelwahed, S. H.; Stevenson, C. D.; Reiter, R. C.; Kiesewetter, M. K. *J. Phys. Chem. B* **2006**, *110*, 1536.

(7) (a) Gerson, F.; Kowert, B.; Peake, B. M. *J. Am. Chem. Soc.* **1974**, *96*, 118. (b) Also see: Rathore, R.; Abdelwahed, S. H.; Guzei, I. A. *J. Am. Chem. Soc.* **2003**, *125*, 8712.

(8) (a) Peters, S. J.; Kiesewetter, M. K.; Turk, M. R.; Stevenson, C. D. *J. Am. Chem. Soc.* **2003**, *125*, 11264. (b) Kiesewetter, M. K.; Reiter, R. C.; Stevenson, C. D. *J. Am. Chem. Soc.* **2004**, *126*, 8884.

(9) (a) It is known that a single broad EPR line verifies the presence of a polymerizing radical during the anionic polymerization, the “living polymer,” such as that from 9-vinylanthracene. (b) Eisenberg A.; Rembaum, A. *Polym. Lett.* **1964**, *2*, 157. (c) Moacanin, J.; Rembaum, A. *Polym. Lett.*, **1964**, *2*, 979. (d) Szwarc, M. *Carbanions, Living Polymers, and Electron-Transfer Processes*; John Wiley and Sons: New York, 1968.

(10) Stevenson, C. D.; Wagner II, E. P.; Reiter, R. C. *J. Phys. Chem.* **1993**, *97*, 10585.

(11) Rathore, R.; Chebny, V. J.; Abdelwahed, S. H. *J. Am. Chem. Soc.* **2005**, *127*, 8012.

(12) The binding constants of  $\text{Na}^+$  and  $\text{Cs}^+$  to 18-crown-6 are comparable; only  $\text{Cs}^+$  is extracted due to its near perfect fit within the cavity of  $2^{\ominus}$ . See: Manege, L. C.; Takayanagi T.; Oshima M.; Motomizu S. *Analyst* **2000**, *125*, 1928.

(13) B3LYP calculations, which reliably predict spin densities, cannot accommodate the large alkali metals.

(14) Neher, E.; Sakmann, B. *Nature* **1976**, *260*, 799. (b) Nelson, D. L.; Cox, M. M. *Lehninger Principles of Biochemistry*, 4th ed.; Freeman, New York, 2005; p 410.

(15) Stevenson, C. D.; Kim, Y. S. *J. Am. Chem. Soc.* **2000**, *122*, 3211.